



Original Article

Geological structure and origin of the Kaochaison hot spring in Phattalung, Southern Thailand

Sukrit Jonjana², Worawut Lohawijarn² and Helmut Dürrast^{1*}

¹ *Geophysics Research Center, Department of Physics, Faculty of Science,*

² *Formerly at the Department of Physics, Faculty of Science,
Prince of Songkla University, Hat Yai, Songkhla, 90112 Thailand.*

Received 15 December 2009; Accepted 11 April 2012

Abstract

Geophysical measurements were conducted in the Kaochaison hot spring area in southern Thailand. The purpose of this work is to determine subsurface geological structures related to the hot spring. Ninety-five gravity points and thirty-seven resistivity soundings were measured in the study area. A positive gravity anomaly is observed in the same area of high resistive bedrock over the Kaochaison hot spring. Both anomalies have an elongated shape with its major axis in N010W direction. A shallow Permian limestone of about 1 km thickness was modeled to explain this positive gravity anomaly. This Permian limestone is likely to be a part of a horst and graben structure related to the regional tectonics and the normal faults act as pathways of the hot waters from a deeper heat source.

Keywords: Hot spring, gravity anomaly, resistivity sounding, horst and graben, Phattalung

1. Introduction

The Kaochaison hot spring is in Ban Kaochaison, Kaochaison District of Phattalung Province, about 840 km south of Bangkok or about 25 km southeast of Phattalung City. In Phattalung Province, there are all together four hot spring sites: the Kaochaison hot spring (PL01) in Kaochaison District with a surface temperature of about 57°C; the Ban Lo Chan Kra hot spring (PL02) in Tamod District with a surface temperature of about 46°C; the Ban Na Thung Pho hot spring (PL03) in Kongra District with a surface temperature of about 50°C; and the Ban Ra Wang Khua hot spring (PL04) in Khuan Khanun District with a surface temperature of about 42°C. The hot springs are the surface manifestation of a geothermal system, which might be used as a renewable energy

source that can be applied to compensate traditional energy resources for recreational, heating, agricultural, industrial, tourism and electricity purposes. Thailand has many hot spring sites, from the North to the South, providing a potential source for renewable energy. In order to utilize this energy a better understanding of the subsurface geology of the geothermal system is required, which is the objective of this study.

2. Geology of the Study Area

The general geology of Kaochaison hot spring and its vicinity is shown in Figure 1. The rocks exposed in the study area range from Cambrian to Quaternary. The Cambrian rocks of Tarutao Group comprise white to light gray colored fine grained sandstone and quartzite. The Ordovician rocks of Thung Song Group compose of mainly gray colored, finely crystalline to coarse grain limestones. The Silurian-Devonian rocks of Pa-Samed Formation are black shales and mudstones. The Carboniferous rocks of Khuan Klang Formation compose of gray colored mudstone, siliceous mudstone, shale, chert

* Corresponding author.
Email address: helmut.j@psu.ac.th

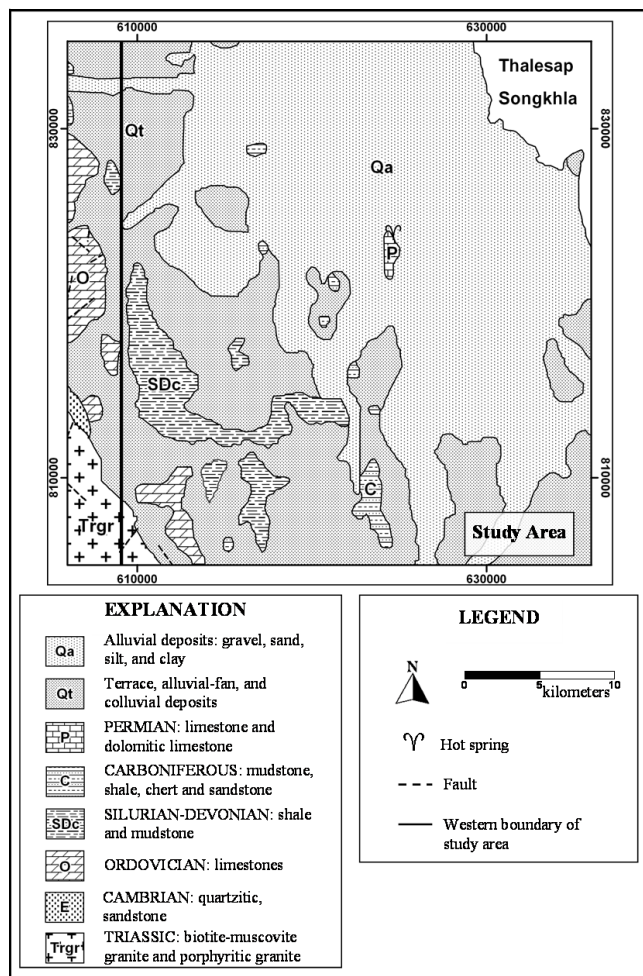


Figure 1. Geological map of the study area (after DMR, 2007).

and sandstone. The Permian rocks of Ratburi Group occur as isolated hills in the eastern part of the study area. The rocks comprise mainly white limestone and dolomitic limestone. The Jurassic-Cretaceous rocks of Lam Thap Formation compose of arkosic sandstone, siltstone and conglomerate. The Quaternary sediment comprises gravel, sand, silt, clay. Intrusive igneous rocks are in Triassic period. They are mainly biotite-muscovite granite and porphyritic granite. The rocks occur in large area as isolated hills in the western part of Phattalung Province with north-south strike direction. They might be heat sources of the geothermal system in the study area (DMR, 2007). Major structures in the study area are the NE-SW and NW-SE trending faults and fractures observed in the Ordovician rocks, Silurian-Devonian rocks and the Triassic granite in the western part of the study area according to DMR (2007).

SE Asia is located in the southeastern part of the Eurasian plate, with the east-dipping subduction of Indo-Australian plate to the east and the south, and the west-dipping Philippine Sea plate and West Pacific plate to the west. It is currently accepted that the present-day tectonic

activity of SE Asia has been governed by the interaction of Indo-Australian plate with Eurasian plate since the time that the India continent collided drastically with Asia during approximately 55 Ma (Packham, 1993). This has caused anti-clockwise rotation of South China plate and a commencement of an extrusion of continental SE Asia southeastward. Such a mega-change in tectonic style may have initiated the major, rift-generating, tensional, pull-apart basins of SE Asia, e.g. Andaman Sea, Gulf of Thailand and South China Sea. The present-day tectonics in continental SE Asia is manifested by the involvement of geothermal resources and neotectonically moderate to strong earthquake activities (e.g. Phuong, 1991, Charusiri *et al.*, 1996).

Sawata *et al.* (1983) conducted Quaternary geological studies in southern Thailand and concluded that the N-S trending basins, located between longitudes $100^{\circ} 15'$ and $100^{\circ} 30'$ E and extending from the coast east of Nakhon Si Thammarat to the Thai-Malaysian border are graben structures, whereas the hill range and the neighboring small basins to the east of the graben structures are horst structures. These horst and graben structures may be the southern extension of geological structures formed by block faulting which trapped oil and natural gas deposits under sediments in the Gulf of Thailand.

Raksaskulwong and Theinprasert (1995) suggested that hot springs in Thailand might be associated with granitic rocks, which are heated by the decay of anomalously high content of radioactive elements in them, or, associated with active fault zones, which accumulate heat due to leakage and circulation of heat from deeper and hotter zones. Whereas Charusiri *et al.* (2000) suggested that the occurrence of geothermal fields are controlled by tensional and strike-slip tectonics in association with seismically active faults and shallow to deep igneous bodies.

3. Geophysical Investigations

In general, geophysical methods utilize contrasts in physical properties of rocks in delineating subsurface geological structures of any study area. The common geophysical methods used for geothermal investigation are gravity method (e.g. Donnell *et al.*, 2001; Khawtawan *et al.*, 2004; Cassidy *et al.*, 2007; Khawdee *et al.*, 2007) and electrical resistivity method (Thongchit and Thamvitawas, 1983; Majumdar *et al.*, 2001). Both, gravity and resistivity measurement were carried out in this study. In gravity measurement, subsurface geology is investigated based on variations in the Earth's gravitational field generated by differences in density among subsurface rocks (Kearey *et al.*, 1991), whereas in the resistivity method, artificially generated electric currents are injected into the ground and the resulting potential differences are measured at the ground surface. In the present study, vertical electrical sounding measurement was used in determining shallow geological structures.

3.1 Gravity measurements

The gravity values of each measuring point were measured with a LaCoste and Romberg gravimeter, model G-565. Ninety-five measuring points were placed along roads available in the study area. The spacing between measuring points was 2 km. Gravity measurement was conducted in leap-frog loops with a closing loop period of 2 to 3 hours for the return to the (intermediate) base station. The location of a measuring point was determined with a Trimble Pathfinder basic-plus GPS. The elevation of a gravity point was measured with an American Paulin altimeter, MDM-5, with an accuracy of ± 0.25 m, corrected for temperature (Figure 2a). The main base station was at 665699 E 774900 N, Zone 47, WGS-84 at the Prince of Songkla University in Hat Yai, Songkla with an absolute gravity value of 9,781,219.8 g.u. or $\mu\text{m/s}^2$. The measured gravity values were corrected for the (1) effects of instrumental drift and tides, (2) latitude, (3) elevation, (4) effects of the mass related to the elevation, and (5) for the surrounding terrain to a datum of mean sea level (e.g. Telford *et al.*, 1998). The corrected data is called Bouguer anomaly.

(1) *Drift correction*: Gravity data drift within one loop of measurements due to time related changes of the gravimeter spring and earth tides. Therefore gravity measurement was repeated after 2 to 3 hours at the same (intermediate) base station. The drift related gravity values for the measurements in-between the two base station readings were linearly interpolated.

(2) *Latitude correction*: As the earth is not a perfect sphere, flattened at the poles, and the earth is rotating around itself (centrifugal forces), the gravity changes significantly with latitude. The International Association of Geodesy (IAG) determined the absolute gravity at mean sea level of the earth represented by a reference ellipsoid, where the pole axis is the shorter one. Equation 1 represents the ellipsoid according to the Geodetic Referencing System in 1980 (GRS-80 Telford *et al.*, 1998):

$$g_{\phi} = 9780318 \times (1 + 0.0053024 \sin^2 \phi + 0.0000059 \sin^2 2\phi) \quad (1)$$

where g_{ϕ} is the gravity in g.u. at latitude ϕ in degrees.

(3) *Elevation correction*: Gravity decreases with increasing elevation. In order to compare all gravity values they are projected to the sea level as datum level. Therefore, each gravity value has to be corrected for elevation, using the American Paulin altimeter values determined for each gravity station (see above). The free-air correction (FAC, in g.u.) is defined by Equation 2 (Telford *et al.*, 1998) with

$$FAC = 3.072 \times h \quad (2)$$

where h is the height of measuring station above the datum level in meter.

(4) *Bouguer Correction*: The Bouguer correction (BC) corrects the effect from the attraction of the mass between the gravity station and the datum level (sea level). It must be subtracted from the observed gravity if the station is above the datum level and added if it is below following Equation 3 (Telford *et al.*, 1998):

$$BC = 0.0004191 \times \rho \times h \quad (3)$$

where BC is the Bouguer correction in g.u., ρ is density of mass in kg/m^3 and h is height of measuring station above the datum level in meter. In this study an average density of $2,500 \text{ kg/m}^3$ was used as the mass above sea level comprises of sediments and hard rock (see Figure 1 and 3a).

(5) *Terrain Correction*: The terrain correction (TC) accounts for the topographic effect in the vicinity of a gravity station. TC was applied by using the Hammer chart (see Telford *et al.*, 1998), which is divided by radial lines into zones (B to J, from the gravity station, at A, outwards) and concentric lines into a certain number of compartments. The elevation difference between the gravity station and each compartment is determined in the field for Zone B-C (max. radius 53.3 m), and using a topographic map for the zones D to J (max. radius 6,652.2 m). The effect of each compartment on the gravity is determined by Equation 4:

$$T = 0.0004191 \frac{\rho}{n} \left(r_2 - r_1 + \sqrt{r_1^2 + z^2} - \sqrt{r_2^2 + z^2} \right) \quad (4)$$

where T is the terrain correction of a compartment in g.u., ρ is the Bouguer correction density in kg/m^3 , n is the number of compartments in a zone, r_1 is the inner radius of a zone in meter, r_2 is the outer radius of a zone in meter, z is the eleva-

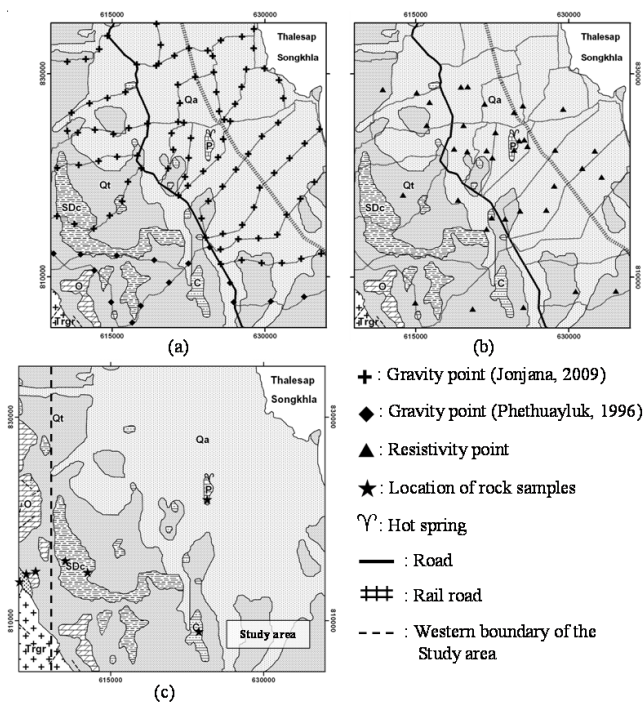


Figure 2. (a) Location of gravity measuring station. (b) Location of resistivity measuring stations. (c) Location where rock samples were taken.

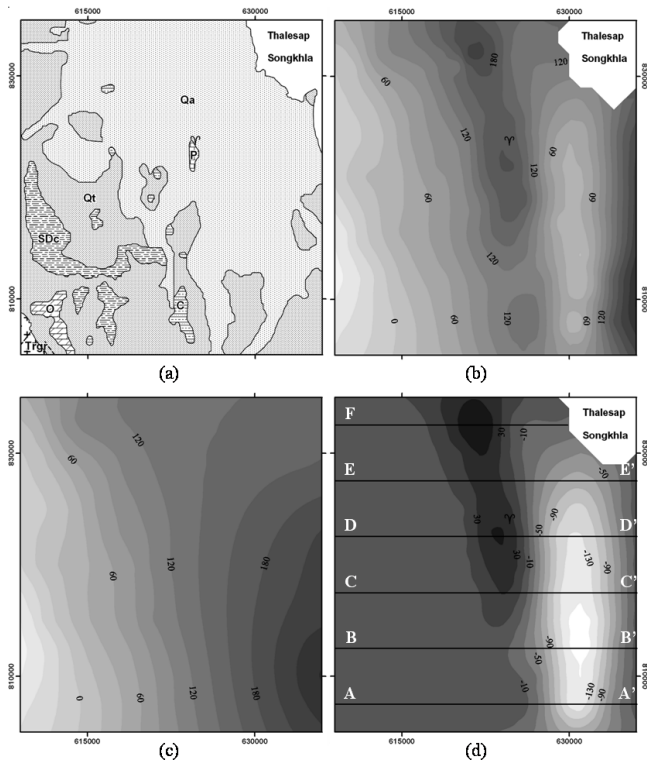


Figure 3. (a) Geological map of the study area. (b) Bouguer anomaly map with contour interval of 20 g.u. (c) Regional gravity anomaly map with contour interval of 20 g.u. (d) Location of profiles superimposed on residual anomaly map with contour interval of 20 g.u..

tion difference in meter between observation point and mean elevation of a compartment (see Kearey *et al.*, 2002). The terrain correction is computed by summing up the gravitational contributions of all compartments.

The final Bouguer anomaly was obtained after all corrections were done following Equation 5

$$g_B = g^{Abs} - g_\phi + FAC - BC + TC \quad (5)$$

where g_B is Bouguer anomaly in g.u., g^{abs} is absolute gravity in g.u. at a measuring station, g_ϕ is the reference gravity in g.u. at latitude, FAC is the Free-air correction in g.u., BC is the Bouguer correction in g.u., and TC is the terrain correction. The final Bouguer anomaly map with interpolated lines of same anomaly values is produced with Surfer, ver. 8.0 (Figure 3b).

3.2 Vertical electrical sounding

Thirty-seven electrical resistivity soundings with Schlumberger electrode configuration were conducted in the study area. The maximum spacing between current electrodes was carried out at 700 meters (Figure 2b). The ground resistance was measured with the ABEM Terrameter SAS-1000 and the Resist program (Velpen, 1988) was used for 1-D modeling of the sounding data.

3.3 Density of rock samples

Hand specimens of less than 3 kg each of six rock-types exposed within and in vicinity of the study area were collected for density determination (Figure 2c). Their bulk densities were determined in the PSU geophysics laboratory. The densities of rocks determined from this and a previous study (Phethuayluk, 1996) were used as constraints in the following gravity modeling. They are 2,770 kg/m³ for the Permian limestone, P, 2,250 kg/m³ for Jurassic-Triassic sandstone, Jk, and 1,800 kg/m³ for Quaternary sediments, Q, and 2,580 kg/m³ for average density of the surrounding rock, which composes of Carboniferous sandstone, Devonian-Silurian mudstone (SDc) and Ordovician limestone.

3.4 Gravity modeling

For further gravity modeling a regional gravity map was calculated from the Bouguer gravity anomaly map comprising data in a 15 km grid from the border of the study area and from within. The calculations and the presentation of the final map of the regional gravity anomaly were done with Surfer, ver. 8.0 (see Figure 3c). The residual Bouguer gravity map was then calculated as the difference between the Bouguer gravity anomaly map and the regional gravity map using Surfer, ver. 8.0 (see Figure 3d). This map was then used for further quantitative gravity modeling. Six lines in E-W direction, AA' (807500 N, Zone 47, UTM WGS-84), BB' (812500), CC' (817500), DD' (822500), EE' (827500), FF' (832500), were chosen for the 2D gravity modeling using the Geo Vista AB-GMM software, version 1.31 (see Figure 3d).

4. Results and Discussion

The Bouguer anomaly map and the geological map of study area are shown in Figure 3. Generally the Bouguer anomaly of the study area increases eastward, i.e., low Bouguer anomaly of -96 g.u. was observed near granitic outcrops in the western part of study area whereas high Bouguer anomaly of 337 g.u. was observed on Quaternary sediment in the eastern part of the study area. In addition, an anomaly of elongated shape trending N010W with amplitude of 120 to 220 g.u. was observed on Permian limestone in the central part and Quaternary sediment in the northern part of the study area. Moreover, low Bouguer anomaly of elongated shape trending N-S with an amplitude of 20 to 120 g.u. was observed in an area covered by Quaternary sediments to the east of the high Bouguer anomaly band.

The resistivity maps at different depths of penetration or the depth-slice resistivity maps of the study area are shown in Figure 4(a). A zone of high resistivity was observed in the same area as that of high Bouguer anomaly in the central part of the study area, whereas that of low resistivity corresponds with that of low Bouguer anomaly in the eastern part of study area. These indicate that the causative body of the geophysical anomaly in the central part of the study area

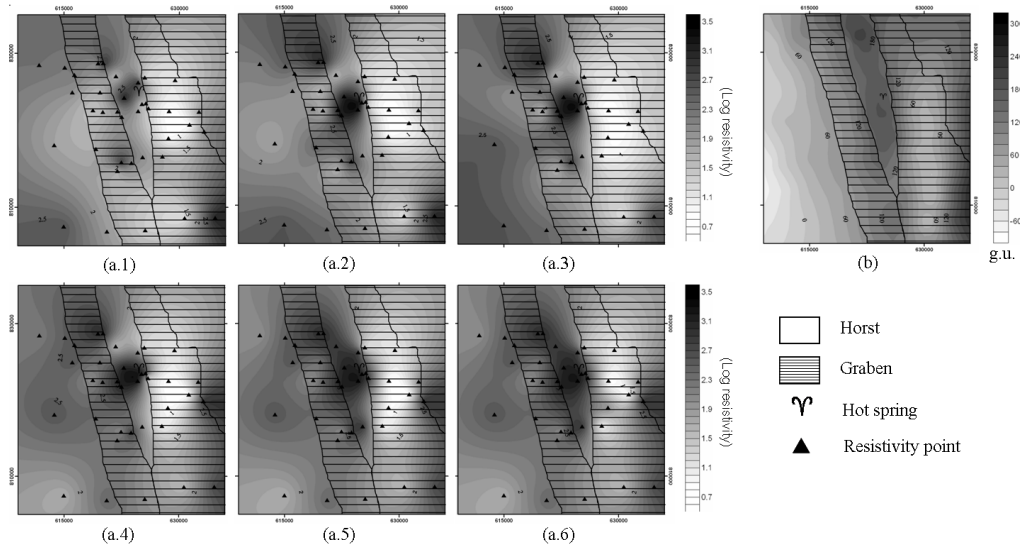


Figure 4. (a) Depth-slice resistivity map superimposed on horst and graben structure map (after Sawata *et al.*, 1983): (a.1) 25 m, (a.2) 50 m, (a.3) 75 m, (a.4) 100 m, (a.5) 125 m, (a.6) 150 m and (b) Bouguer anomaly map superimposed on the horst and graben structure map (after Sawata *et al.*, 1983).

should have higher density and be more resistive than its surrounding rocks and Permian limestone is the most preferable one. It could be also observed that the hot spring PL01 is at the contact of high and low resistivity zones. Moreover, the high Bouguer anomaly zone in the central part and low Bouguer anomaly in the eastern part of the study area correspond with the horst and graben structures proposed by Sawata *et al.* (1983) as shown in Figure 4(b). The regional gravity anomaly of the study area increases eastward with a gradient of 9.8 g.u./km and the contour of this regional gravity anomaly is shown in Figure 3(c).

Quantitative interpretation of Bouguer anomaly was carried out in order to determine subsurface geological structures in vicinity of hot spring PL01. The interpretation was made with forward gravity modeling on six gravity profiles namely; AA', BB', CC', DD', EE', and FF' (Figure 3d).

Gravity anomaly and subsurface geological model of the profile AA' are shown in Figure 5. Jurassic-Cretaceous rocks of 800 meters thickness underlying Quaternary sediments of 200 meters thickness at 626000-636000 E (Figure 5b) were modeled to explain the low residual anomaly of about -139 g.u. at 626000-636000E (Figure 5a).

Gravity anomaly and subsurface geological model of the profile BB' are shown in Figure 6. Again in this profile, Jurassic-Cretaceous rocks of 800 meters thickness underlying Quaternary sediments of 200 meters thickness at 624500-636000 E were modeled to explain the low residual anomaly of about -162 g.u. at 624500-636000 E (Figure 6b).

Gravity anomaly and subsurface geological model of the profile CC' are shown in Figure 7. In this profile, Permian limestone of about 950 m thickness underlying Quaternary sediments at depths 85 meters was modeled to explain the high residual anomaly of about 31 g.u. at 621000-626000 E, whereas Jurassic-Cretaceous rocks of 800 meters thickness

underlying Quaternary sediments of 200 meters thickness at 624500-636000 E were modeled to explain the low residual anomaly of about -146 g.u. at 626000-636000 E (Figure 7b).

Gravity anomaly and subsurface geological model of the profile DD' are shown in Figure 8. Permian limestone of 1,000 m thickness was modeled to explain the high residual anomaly of about 57 g.u. at 620000-626000 E, whereas Jurassic-Cretaceous rocks of 850 meters thickness underlying Quaternary sediments of 150 meters thickness were modeled to explain the low residual anomaly of about -131 g.u. at 626000-636000 E (Figure 8b).

Gravity anomaly and subsurface geological model of the profile EE' are shown in Figure 9. Permian limestone of about 920 m thickness underlying Quaternary sediments at depths 80 meters was modeled to explain the high residual anomaly of about 38 g.u. at 618000-626000 E, whereas Jurassic-Cretaceous rocks of 325 meters thickness underlying Quaternary sediments of 125 meters thickness were modeled to explain the low residual anomaly of about -80 g.u. at 626000-636000 E (Figure 9b).

Gravity anomaly and subsurface geological model of the profile FF' are shown in Figure 10. Permian limestone of about 980 m thickness underlying Quaternary sediments at depths 20 meters was modeled to explain the high residual anomaly of about 69 g.u. at 616000-625000 E, whereas Jurassic-Cretaceous rocks of 35 meters thickness underlying Quaternary sediments of 65 meters thickness were modeled to explain the low residual anomaly of about -13 g.u. at 626000-628000 E (Figure 10b).

The resistivity models obtained from electric sounding measurements were compared with interpreted geological cross-sections obtained from gravity models at shallow depth along four parallel lines, which are shown in Figure 11, namely, AA', CC', DD', and EE'. These integrated models are

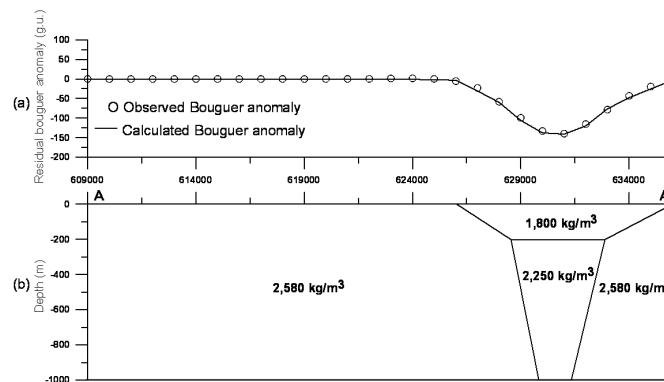


Figure 5. (a) Observed and calculated Bouguer anomaly (g.u.) along profile AA'. (b) Geological model along profile AA' used for calculating the Bouguer anomaly (see a). The values indicate the density values used in each segment of the profile.

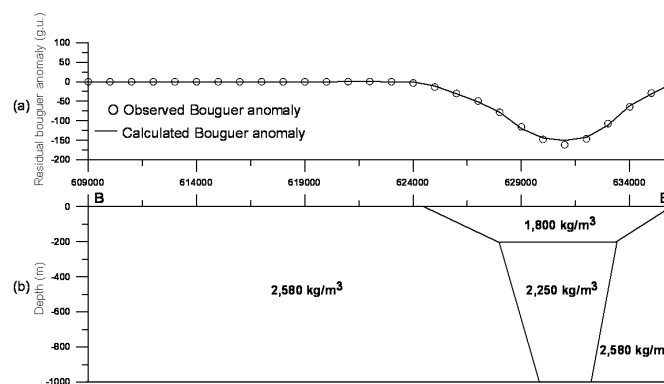


Figure 6. (a) Observed and calculated Bouguer anomaly (g.u.) along profile BB'. (b) Geological model along profile BB' used for calculating the Bouguer anomaly (see a). The values indicate the density values used in each segment of the profile.

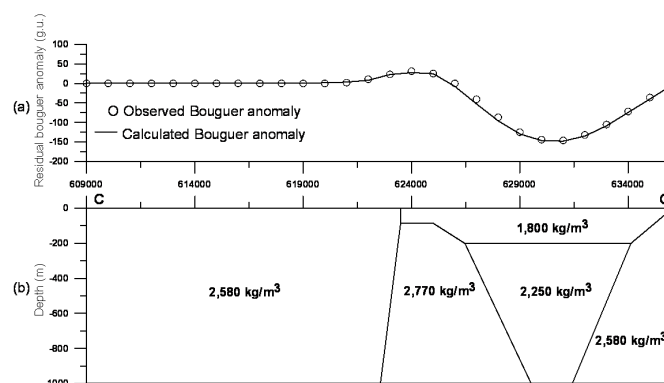


Figure 7. (a) Observed and calculated Bouguer anomaly (g.u.) along profile CC'. (b) Geological model along profile CC' used for calculating the Bouguer anomaly (see a). The values indicate the density values used in each segment of the profile.

presented in Figure 12.

Along line AA', the thickness of the modeled Quaternary sediments, 80 meters, agrees with the thickness of a conductive layer 38 Ohm-m, observed at the sounding point "P36" on the eastern part of the profile (Figures 12a).

Along line CC', the depth to Permian limestone was modeled to correspond with the depth of 100 meters to the

resistive substratum, 769 Ohm-m, at point "P29" in the central part of the profile. In addition, the thickness of Quaternary sediments, 65 meters, was modeled in agreement with the thickness of a near-surface conductive layer, 11 Ohm-m, at point "P30" on the eastern part of the profile (Figures 12b).

Along line DD', the depths to Permian limestone was modeled in agreement with the depths of 33 to 107 meters to

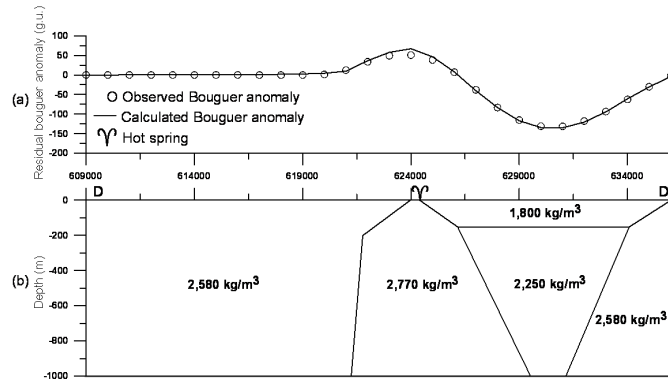


Figure 8. (a) Observed and calculated Bouguer anomaly (g.u.) along profile DD'. (b) Geological model along profile DD' used for calculating the Bouguer anomaly (see a). The values indicate the density values used in each segment of the profile.

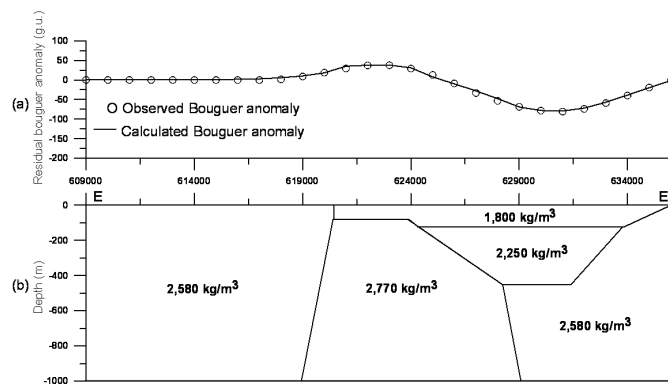


Figure 9. (a) Observed and calculated Bouguer anomaly (g.u.) along profile EE'. (b) Geological model along profile EE' used for calculating the Bouguer anomaly (see a). The values indicate the density values used in each segment of the profile.

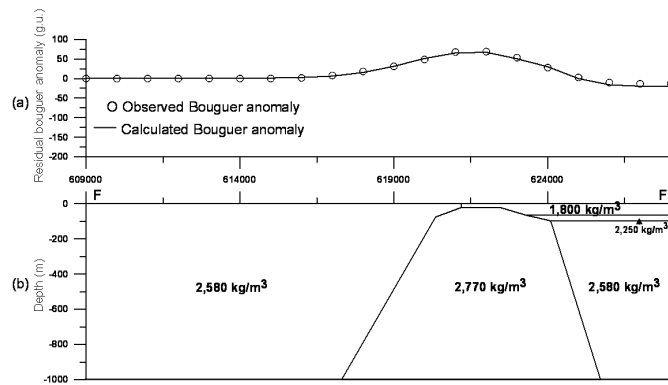


Figure 10. (a) Observed and calculated Bouguer anomaly (g.u.) along profile FF'. (b) Geological model along profile FF' used for calculating the Bouguer anomaly (see a). The values indicate the density values used in each segment of the profile.

the resistive substratum of 600 to 1,505 Ohm-m at points P01 and P02 in the central part of the profile. In addition, the thickness of Quaternary sediments was modeled to correspond with the thickness of 100 to 200 meters of the near-surface conductive layer, 20 to 90 Ohm-m, at point P06 and P18 in the eastern part of the profile as shown in Figures 12(c).

Along line EE', the depth to Permian limestone was

modeled in agreement with the depth of 111 to 124 meters to a high resistive substratum, 588 to 800 Ohm-m, at points "P11" and "P28" in the central part of the profile. In addition, the thickness of the Quaternary sediments was modeled to correspond with the thickness of 158 meters of the near-surface conductive layer, 30 Ohm-m, at point "P12" in the eastern part of the profile (Figures 12d).

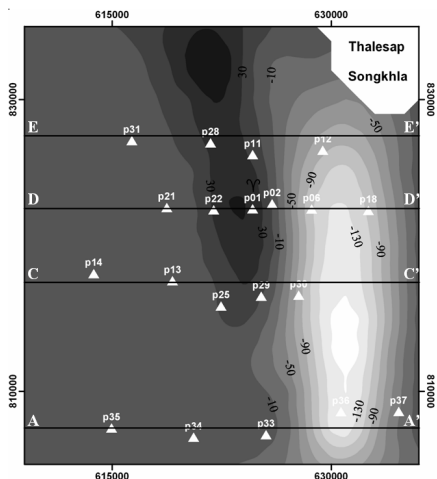


Figure 11. Location of profiles (AA', CC', DD', and EE') superimposed on residual anomaly map. p01 to p37 are the locations of the vertical sounding measurements.

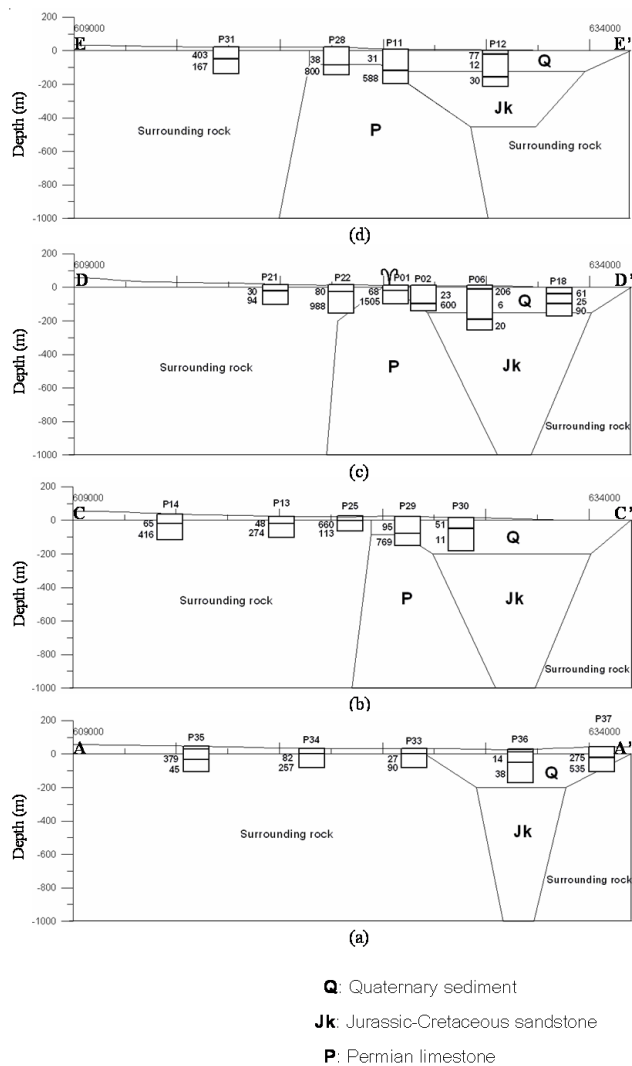


Figure 12. Resistivity models incorporated in the geological models from the gravit modeling for the profile (a) AA', (b) CC', (c) DD' and (d) EE' (from bottom to top)

5. Discussion and Conclusion

Geological structures beneath the hot spring area named PL01 in Khao Chaison were determined from gravity and resistivity sounding measurement, where the resistivity data provide more detailed information about the shallow subsurface, mainly the thickness of the less resistive Quaternary sediments and higher resistive rocks. The gravity measurements and modeling provide information about the intermediate and deeper subsurface. Both geophysical methods applied in this study carry a certain degree of uncertainty (see for example Kearey *et al.*, 1991). The resistivity interpretation is not directly verified by borehole data; however no detailed interpretation of the different layers with different resistivity values was required for this study. The residual Bouguer anomaly values are derived based on certain assumptions, e.g. the density value of the Bouguer correction, or the determination of the regional gravity trend, whereas the quantitative 2D modeling required an initial geological model. As outlined above this model, especially the horst and graben tectonics, was developed from the geological map information and previous work done by Sawata *et al.* (1983), and it fits into the regional geological and tectonic model (see Section 2). However, uncertainties still remain, as they are part of the applied geophysical methods.

The integration of all data and available information provides following picture of the subsurface geology in the study area. In the central part of the area where the Khao Chaison hot spring situates a N010W trending strip of 70 g.u. residual Bouguer anomaly was observed. A shallow Permian limestone of about 1,000 m thickness was modeled to explain this positive residual anomaly. In addition, Jurassic-Cretaceous rocks of 800 meters thickness underlying Quaternary sediments of 200 meters thickness were modeled to explain a strip of -160 g.u residual Bouguer anomaly to the east of the positive residual Bouguer anomaly. The depths to Permian rocks were modeled to conform with the depths to resistive substrata obtained from the resistivity measurement.

It could be seen that the Khao Chaison hot spring lies at the contact between high and low resistivity zones in the depth-slice resistivity map. The locations of these modeled Permian limestone and Jurassic-Cretaceous rocks correspond very well with the locations of the proposed horst and graben structures, which are the westward extension of the horst and graben structures developed in the Gulf of Thailand (Sawata *et al.*, 1983). It is likely that modeled normal faults which bound the horst and graben structure in the study area and fractures in the Permian limestone act as pathways for the hot waters of hot springs from a deeper heat source (Figure 13).

Acknowledgments

The authors would like to thank the Graduate School of the Prince of Songkla University for a research grant. Thanks also to the International Program in the Physical Sciences of

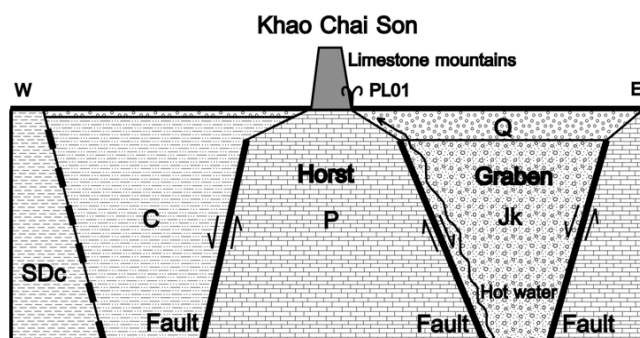


Figure 13. Schematic W-E cross-section of the study area showing the proposed horst and graben structure. The hot water flows from a deeper heat source to the surface along the faults separating horst and graben, PL01 = hot spring, Q = Quaternary sediment, Jk = Jurassic-Cretaceous sandstone, P = Permian limestone

Uppsala University, Sweden, for research equipment and interpretation software.

References

- Cassidy, J., France, S. and Locke C. 2007. Gravity and Magnetic investigation of maar volcanoes, Auckland volcanic field, New Zealand. *Journal of Volcanology and Geothermal Research*. 159, 153-163.
- Charusiri, P., Daorerk, V. and Supajanya, T. 1996. Applications of Remote-sensing techniques to geological structures related to earthquakes and earthquake-prone areas in Thailand and neighboring areas: A preliminary study. *Journal of Scientific Research, Faculty of Science, Chulalongkorn University, Bangkok*. Vol. 21 (1), pp. 23-43.
- Charusiri, P., Chaturongkavanich, S., Takashima, I., Kosuwan, S., Won-In, K. and Ngo Ngoc, C. 2000. Application of Geothermal Resources of Thailand, Vietnam, and Myanmar to tectonic settings. *Proceedings of the World Geothermal Congress, Kyushu-Tohoku, Japan, organized by the International Geothermal Association, May 28-Jun 10, 2000*.
- Department of Mineral Resources (DMR) 2007. *Geology and Geological Resources of Phattalung*. Bangkok. Department of Mineral Resources (in Thai).
- Donnell, T. M., Miller, K.C. and Witcher, J.C. 2001. A seismic and gravity study of the McGregor geothermal system, southern New Mexico. *Geophysics*. 66, 1002-1014.
- Kearey, P., Brooks, M. and Hill, I. 2002. *An Introduction to Geophysical Exploration*. 4th ed. Blackwell Science, London, UK, pp. 119-173
- Khawdee, P. 2007. *Geophysical Study of Geothermal Resources in Kanchanadit and Ban Na Doem Distric, Surat Thani Province*. Master of Science Thesis in Physics, Prince of Songkla University, Songkhla, Thailand, pp. 83-84.
- Khawtawan, A., Lohawijarn, W. and Tonnayopas, D. 2004. Gravity Anomaly of Chaiya Geothermal Area. *International Conference on Applied Geophysics, Chiang Mai, Thailand, November 26-27, 2004*, pp. 15-21.
- Majumdar, R.K., Majumdar, N. and Mukherjee, A.L. 2000. Geoelectric investigations in Bakreswar geothermal area, West Bengal, India. *Geophysics*. 45, 187-202.
- Packham, G.H. 1993. Plate tectonics and the development of sedimentary basins of the dextral regime in western southeast Asia. *Journal of Southeast Asian Earth Sciences*. 8, 497-511.
- Phethuayluk, S. 1996. *A Regional Study of Geological Structure in Changwat Songkhla, Changwat Phattalung and Changwat Trang with Geophysical Method*, Master of Science Thesis in Physics, Prince of Songkla University, Songkhla, Thailand, pp. 51-57.
- Phuong, N.I-I. 1991. Probabilistic assessment of earthquake hazard in Vietnam based on seismotectonic regionalization. *Tectonophysics*. 198, 81-93.
- Raksaskulwong, M. and Thienprasert, A. 1995. Heat flow studies and geothermal energy development in Thailand. In M.L. Gupta and M. Yamano, editors. *Terrestrial heat flow and geothermal energy in Asia*. New Delhi. Oxford and India Book House (I.B.H.) Publishing, pp. 129-144.
- Sawata, H., Wongsomsak, S., Tanchotikul, A., Darnsawasdi, R. Maneeprapun K. and Muenlek, S. 1983. A hypothetical idea on the formation of Hatyai basin and the Songkhla lagoon. *Proceeding of the Annual Technical Meeting 1982, Department of Geological Sciences, Chiang Mai University, 1-2 Feb 1983*, 109-112.
- Telford, W.M., Geldart, L.P. and Sheriff, R.E. 1998. *Applied Geophysics*. 2nd ed. Cambridge University Press, Cambridge, UK, pp. 10-19.
- Thongchit, P. and Thammavittawat, S. 1983. A report on geophysical survey with electrical resistivity in the geothermal area of Tumbol Pongkum, Amphoe Doi Saket, Changwat Chiangmai, *Geophysics Section, Economic Geology Division, Department of Mineral Resources, Bangkok, Thailand*, pp. 18 (in Thai).
- Velpen, V., 1988. RESIST Version 1.0. ITC, ITC, Faculty of Geo-Information Science and Earth Observation of the University of Twente, The Netherlands.